

# Analytical Study of the IEEE 802.11p MAC Sublayer in Vehicular Networks

Chong Han, *Student Member, IEEE*, Mehrdad Dianati, *Member, IEEE*, Rahim Tafazolli, *Senior Member, IEEE*, Ralf Kernchen, and Xuemin (Sherman) Shen, *Fellow, IEEE*

**Abstract**—This paper proposes an analytical model for the throughput of the enhanced distributed channel access (EDCA) mechanism in the IEEE 802.11p medium-access control (MAC) sublayer. Features in EDCA such as different contention windows (CW) and arbitration interframe space (AIFS) for each access category (AC) and internal collisions are taken into account. The analytical model is suitable for both basic access and the request-to-send/clear-to-send (RTS/CTS) access mode. Different from most of existing 3-D or 4-D Markov-chain-based analytical models for IEEE 802.11e EDCA, without computation complexity, the proposed analytical model is explicitly solvable and applies to four access categories of traffic in the IEEE 802.11p. The proposed model can be used for large-scale network analysis and validation of network simulators under saturated traffic conditions. Simulation results are given to demonstrate the accuracy of the analytical model. In addition, we investigate service differentiation capabilities of the IEEE 802.11p MAC sublayer.

**Index Terms**—IEEE 802.11p, performance analysis, vehicular ad-hoc networks (VANETs).

## I. INTRODUCTION

MODERN intelligent transportation systems (ITSs) aim to apply information and communication technologies (ICTs) to improve the quality, effectiveness, and safety of future transportation systems [1]–[3]. It is envisioned that the deployment of advanced ITS technologies will contribute to effective management of traffic in urban areas, as well as improvement of safety on highways and roads. In addition, access to broadband Internet via ITS technologies will enable a variety of infotainment applications that are expected to revolutionize the quality of experience for the passengers and drivers. Vehicle-to-vehicle (V2V), which is alternatively known as car-to-car (C2C) or intervehicle communications (IVC), combined with

Manuscript received September 20, 2011; accepted December 12, 2011. Date of publication February 18, 2012; date of current version May 30, 2012. This work was carried out within DRIVE C2X project which is funded by the European Union's Seventh Framework Program (FP7/2007-2013) under Grant Agreement 270410. The Associate Editor for this paper was L. Yang.

C. Han, M. Dianati, and R. Tafazolli are with the Centre for Communication Systems Research, Department of Electronic Engineering, University of Surrey, GU2 7XH, Surrey, U.K. (e-mail: chong.han@surrey.ac.uk; m.dianati@surrey.ac.uk; r.tafazolli@surrey.ac.uk).

R. Kernchen was with the Centre for Communication Systems Research, Department of Electronic Engineering, University of Surrey, GU2 7XH, Surrey, U.K. He is now with Rulemation Ltd., EC1V 4PW London, U.K. (e-mail: r.kernchen@surrey.ac.uk).

X. Shen is with the Department of Electrical and Computer Engineering, University of Waterloo, Waterloo, ON N2L 3G1, Canada (e-mail: xshen@bbr.uwaterloo.ca).

Color versions of one or more of the figures in this paper are available online at <http://ieeexplore.ieee.org>.

Digital Object Identifier 10.1109/TITS.2012.2183366

vehicle-to-infrastructure (V2I) communications, which is also known as roadside-to-vehicle communications (RVC), are two key enabling components of ITS technologies.

IVCs rely on direct communications between individual vehicles that could enable a large class of road safety and traffic efficiency applications (e.g., collision avoidance, passing assistance, electronic toll collection, smart parking, and platooning) [4]–[8], whereas RVC systems [9] rely only on communication facilities among vehicles and fixed roadside infrastructures. Hybrid vehicular communication (HVC) systems extend the range and functionality of RVC systems by improving the communications range, as well as their functionalities.

HVC systems define special hybrid communication scenarios where both ad-hoc and infrastructure-supported communication modes are possible. This fact suggests that distributed medium-access control (MAC) schemes such as the IEEE 802.11x series could be suitable candidates for the MAC sublayer of the HVC systems. However, the rapidly changing network topologies, the characteristics of propagation environment in HVC systems, and the requirements of specific applications in such networks could be different from those of the traditional networks that rely on the existing MAC sublayers. Thus, the IEEE 802.11p has been proposed for Wireless Access in Vehicular Environments [16].

The IEEE 802.11p uses an Enhanced Distributed Channel Access (EDCA) MAC sublayer protocol designed based on that of the IEEE 802.11e with some modifications to the transmission parameters. The physical layer of the IEEE 802.11p is similar to that of the IEEE 802.11a standard. The IEEE 802.11p supports transmission rates ranging from 3 to 27 Mb/s (payload) over a bandwidth of 10 MHz, which is half of the bandwidth in 802.11a. The IEEE 802.11p aims to provide both V2V and V2I communications in ranges up to 1000 m in a variety of environments (e.g., urban, suburban, rural, and motorway) with relative vehicle velocities of up to 30 m/s. Considering the fast movement and frequent trajectory changes in vehicular ad-hoc networks (VANETs), on the MAC sublayer, frequent handshakes and authorization are expected to be limited to reduce the high rate of link disconnections. Taking the unique characteristics of VANETs into account, low latency and high reliability are required for safety-related applications, whereas high throughput, low packet loss rate, high resource utilization, and fairness vehicles are main concerns for infotainment applications [10]. Hence, different quality-of-service (QoS) metrics should be considered for corresponding categories of ITS applications. In addition, the available location information can help reduce high collision rate on the shared channel. Analytical

modeling on the IEEE 802.11p should reveal the performance and shortcomings of the MAC sublayer in VANETs, from which suitable schemes can be designed for VANETs.

Performance analysis of the IEEE 802.11p MAC sublayer is an important and challenging problem that has been partially investigated in some recent publications. A simulation model for comparison of packet loss versus relative velocity of vehicles for the IEEE 802.11p and 802.11a standards is given in [11]. The presented simulation results indicate that 802.11p outperforms 802.11a in terms of packet loss in a typical vehicular environment. In [12] and [13], simulation-based studies of the performance of the IEEE 802.11p MAC sublayer are given. These papers provide simulation-based studies of the aggregate throughput, the average delay, and the packet loss due to collision in some specific simulation scenarios.

There are a number of related publications that also consider analytical modeling of the MAC sublayer for the IEEE 802.11e. A comprehensive survey of the related publications is provided in Section II. As we discuss there, the existing analytical models for the 802.11e are often computationally prohibitive for studying the MAC sublayer when there are more than two ACs. Motivated by these shortcomings, we propose a computationally tractable analytical model that is customized for the EDCA mechanism of the MAC sublayer of the IEEE 802.11p standard. The proposed model extends the Markov chain analysis in [18] and [27], considering the accurate specifications of the 802.11p standard. The 2-D Markov chain in this paper is generated to model the backoff procedure for each access category (AC) queue. Different CW and arbitration interframe space (AIFS) values for each AC and internal collisions are taken into account. Slots are divided into different zones for deriving the relation between the transmission probability and the collision probability. Finally, an accurate model for the throughput of each AC is derived. Both basic and RTS/CTS access modes are supported in this paper. The proposed model is validated against simulation results to demonstrate its accuracy. In addition, service differentiation performance of the 802.11 MAC sublayer is studied. Finally, we use our verified simulation model to study the performance degradation behavior of the 802.11p MAC sublayer due to high contention when the number of stations is relatively high.

The remainder of this paper is organized as follows: In Section II, a comprehensive survey of the related publications is provided, and the motivation of the research is presented. In Section III, the system model, which includes the relevant aspects of the IEEE 802.11p, is specified. In Section IV, the analytical model for the throughput of EDCA in the IEEE 802.11p MAC sublayer is proposed. Section V validates the accuracy of the proposed model by comparing the analytical and simulation results. This section also includes further study of the performance of 802.11p using our verified simulation model. The summary and the concluding remarks are given in Section VI.

## II. RELATED WORK AND MOTIVATION

Some recent publications [23]–[36] have considered analytical models for EDCA in IEEE 802.11e. The objective of this section is to discuss the main contributions of the existing

publications and highlight the differences and contributions of this paper.

Some of these works are found with low accuracy in predicting throughput. In [23] and [24], the authors propose a delay model that predicts throughput as well; however, as the authors mentioned, the model is found not to be accurate for prediction of throughput in a semisaturated part, compared with the simulation results. Alternative analytical models are also presented in [25] and [26]. However, these papers do not consider internal collisions. Our study indicates that omitting the internal collisions will result in inaccurate calculation of the transmission probabilities.

Robinson and Randhawa [26] proposed an analytical model, using the concept of contention zones, that only considers two ACs without considering internal collisions. Reference [27] uses similar concepts as [26] to propose another model that also considers internal collisions. Clifford *et al.* [28] proposes another model that also considers two ACs. The shortcoming of these works is that they cannot be easily extended to consider four ACs, which is one of the main specifications of 802.11p. Different from these papers, the proposed model in this paper considers four ACs, as specified in the standard.

There is another family of models in the works [29]–[35], which consider four ACs in each station in modeling the IEEE 802.11e. However, most of these 3-D Markov-chain-based analytical models bring unnecessary calculation complexity into the computation of transmission probabilities of different ACs. These models have been validated for the scenarios with two ACs. However, the complexity of the solutions for a scenario with four ACs is prohibitive. Thus, to the best of our knowledge, the existing papers only validated these models for the scenarios with only two ACs. For instance, Kong *et al.* [30] proposed a 3-D discrete-time Markov chain model for multiple ACs per station to model the backoff procedure. However, the model is finally used for only two ACs (i.e., AC1 and AC3) due to the calculation complexity. Similar shortcomings exist in works [31]–[35]. In [36], a 2-D Markov chain is proposed to model each AC in the station. The simulation results show that this model is valid for four access categories of traffic. However, in the proposed Markov chain, the  $PT_i$  variable (i.e., the probability that backoff counter can be decreased by one for access class  $i$ ) is represented by other variables with constraints of “before AIFS[i]” and “after AIFS[i].” This makes the calculation of  $PT_i$  impossible since the backoff timer is randomly chosen every time. Thus, we believe that the key transmission probabilities of different ACs could not be obtained. Xu *et al.* [37] proposed solid work on the access delay model for the IEEE 802.11e EDCA; however, no throughput model is obtained in this paper.

The contributions of our paper with respect to the existing publications can be summarized as follows: Our work aims to propose an analytical model for the IEEE 802.11p MAC sublayer under saturated traffic conditions, taking into account CW and AIFS for different ACs, and an internal-collision-resolving mechanism. In the modeling, strong approximations are avoided to assure the accuracy of our model. Four ACs are considered throughout the analytical modeling and validation, which provides full support to all the ACs in the IEEE

802.11p. Moreover, the proposed model is relatively simple to be explicitly solved for the validation of all four ACs. The proposed analytical model can be used for the analysis of large-scale scenarios or as the validation tool for different network simulators to implement the IEEE 802.11p.

### III. SYSTEM MODEL

The major specifications of the IEEE 802.11p standard that distinguish it from similar standards such as the IEEE 802.11a,e are briefly discussed in this section. We focus on the aspects of the physical (PHY) and MAC sublayers that are relevant to the analysis in this paper.

#### A. PHY Layer in 802.11p

The PHY layer of the IEEE 802.11p is similar to that of the IEEE 802.11a as it operates at 5.9 GHz, which is very close to that of 802.11a at 5 GHz. The PHY layer in 802.11p adopts an orthogonal frequency-division multiplexing transmission technique similar to that of 802.11a; however, the bandwidth of a single channel in 802.11p is scaled down to 10 MHz from that of 802.11a. This is motivated by the characteristics of the propagation environment in HVC systems. Unlike the traditional applications of wireless local area networks, where the velocity of the nodes is relatively low, in a vehicular communication environment, the relative velocity of the nodes could be significantly higher. Thus, the delay spread of multiple paths could be significantly higher, which could exacerbate intersymbol interference when the signal bandwidth is high. As a result, a 10-MHz bandwidth is a reasonable choice for vehicular environments.

#### B. MAC Sublayer in 802.11p

The EDCA proposed in IEEE 802.11e [15] is designed for contention-based prioritized QoS support. The EDCA mechanism defines four ACs that provide support for data traffic with four priorities. Each AC queue works as an independent DCF station (STA) with enhanced distributed channel access function (EDCAF) to contend for Transmission Opportunities (TXOP) using its own EDCA parameters. Fig. 1 shows the prioritization mechanism inside each STA, where there are four transmit queues and four independent EDCAFs for different traffic categories. The value of AIFS for each AC is denoted by  $AIFS[AC]$ . Each AC queue uses different AIFS,  $CW_{min}$ , and  $CW_{max}$ .

Prioritization of transmission in EDCA is implemented by a new interframe space (IFS), i.e., AIFS, which can be considered as an extension of the backoff procedure in DCF. As shown in Fig. 2, aside from the original short interframe spacing (SIFS), PCF IFS (PIFS), and DCF IFS (DIFS), new AIFS values for different ACs are introduced in EDCA. The duration  $AIFS[AC]$  is a duration derived from the value  $AIFSN[AC]$  by the relation in

$$AIFS[AC] = AIFSN[AC] \times aSlotTime + aSIFSTime \quad (1)$$

where  $AIFSN[AC]$  is the value set by each MAC protocol in the EDCA parameter table,  $aSlotTime$  is the duration of a slot time, and  $aSIFSTime$  is the length of SIFS. Different ACs

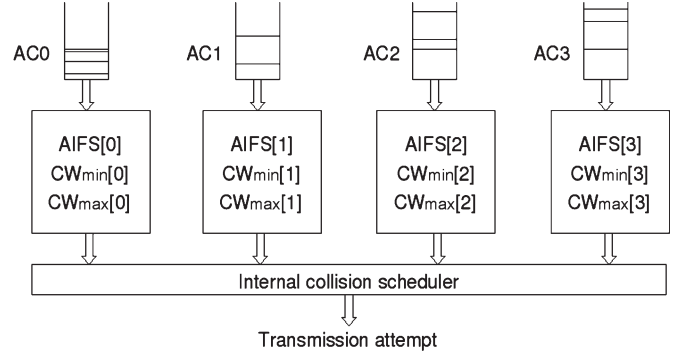


Fig. 1. Prioritization mechanism inside a single STA.

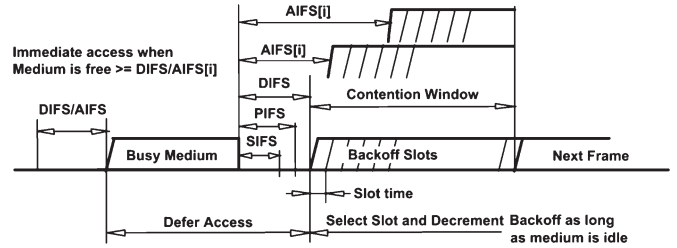


Fig. 2. Some IFS relationships (obtained from [16]).

TABLE I  
DEFAULT EDCA PARAMETERS IN IEEE P802.11p/D8.0

AC	$CW_{min}[AC]$	$CW_{max}[AC]$	AIFSN [AC]
AC <sub>BK</sub>	$CW_{min}$	$CW_{max}$	9
AC <sub>BE</sub>	$(CW_{min} + 1)/2 - 1$	$CW_{max}$	6
AC <sub>VI</sub>	$(CW_{min} + 1)/4 - 1$	$CW_{min}$	3
AC <sub>VO</sub>	$(CW_{min} + 1)/4 - 1$	$(CW_{min} + 1)/2 - 1$	2

are allocated with different AIFSNs. The AC with a smaller AIFS has higher priority to access the channel. In addition, different  $CW_{min}$  and  $CW_{max}$  sizes are assigned to different ACs. Assigning a shorter CW size to a higher priority AC ensures that higher priority AC a higher chance to access the channel than a lower priority AC.

The default EDCA parameter setting for station operation is shown in Table I. According to the latest version of the draft standard of 802.11p [16],  $CW_{min}$  is 15, and  $CW_{max}$  is 1023.

Each station has four AC queues acting as four independent stations. If the channel is sensed idle for the duration of  $AIFS[x]$  and if the  $AC_x$  queue has backlogged data for transmission, the backoff timer for the EDCAF will be checked. Otherwise, the EDCAF shall try to initiate a transmission sequence. If it has a nonzero value, the EDCAF shall decrease the backoff timer. However, since each STA has four EDCAFs, there is a probability that more than one AC queue initiates a transmission sequence at the same time. Hence, a collision may occur inside a single STA. A scheduler inside STAs will avoid this kind of internal collision by granting the EDCA-TXOP to the highest priority AC. At the same time, the other colliding ACs will invoke the backoff procedure due to the internal collision and behave as if there were an external collision on the wireless medium. However, an STA does not set the retry bit in the MAC headers of low-priority queues for internal collisions. An external collision occurs when more than one AC is granted

TXOPs by different STAs. Since there is no priority among STAs, stations have to compete for channel access with equal opportunity. The collided frames will be deferred, and the backoff procedure is invoked.

#### IV. ANALYTICAL MODEL

In this section, a 2-D Markov chain is used to model the backoff procedure for each AC queue. In this model, we only consider the saturated traffic because it helps validate the accuracy of simulators with reduced computation complexity. Nonsaturated traffic is more practical, which is considered in the performance analysis part in Section V. In this section, first, we obtain the transmission probability of each AC queue by analyzing the Markov chain. During the backoff procedure, the time slots are divided into different zones corresponding to different contention periods, as will be explained later. Then, the collision probability of each AC queue is represented as a function of transmission probabilities, and the transmission probabilities for different ACs are calculated. Finally, an accurate model for the throughput of each AC is derived. Both basic and RTS/CTS access modes are taken into account in the proposed model. In the proposed analytical model, the AIFS, CW for different ACs, and the internal collisions inside each station are taken into account. The details of our derivations are given in the following: The analytical model is based on Markov chain analysis in [18]. The aim is to analyze the performance of MAC sublayer; thus, without loss of generality, the packet losses due to the channel errors are excluded. The notations used in the analysis are summarized in Table II.

The 2-D Markov chain representing the dynamic behavior of the EDCA backoff process for an individual AC is shown in Fig. 3. Each state in this chain is represented by the tuple  $[s(t), b(t)]$ , where  $s(t)$  is the backoff stage of a head-of-line (HOL) packet for each AC at time  $t$  that corresponds to the number of collisions that the HOL packet has suffered up to time  $t$ , whereas  $b(t)$  is the backoff counter at time  $t$ . An STA will attempt to transmit the HOL packet whenever the backoff counter  $b(t)$  is zero, regardless of the backoff stage  $s(t)$ . The collision probabilities at different backoff stages are different from each other, e.g., nodes at stage 0 have a larger collision probability than that at stage  $M$ . However, to make the model mathematically tractable, in this paper, the collision probabilities  $R_m$  at all backoff stages are assumed to be the same for each AC.

Let  $(i, j)$  represent the event of being in state  $[s(t) = i, b(t) = j]$  and  $P(i, j|k, l)$  be the probability of transition from state  $(k, l)$  in time  $t$  to state  $(i, j)$  in time  $t + 1$ . The transition probabilities in the Markov chain in Fig. 3 are given in the following:

$$\begin{aligned}
 P(i, k|i, k+1) &= 1, \text{ for } 0 \leq k \leq W_i - 2, 0 \leq i \leq M + f \\
 P(0, k|i, 0) &= \frac{1 - R_m}{W_0}, \text{ for } 0 \leq i \leq M + f - 1 \\
 &\quad 0 \leq k \leq W_0 - 1 \\
 P(0, k|M + f, 0) &= \frac{1}{W_0}, \text{ for } 0 \leq k \leq W_0 - 1 \\
 P(i, k|i-1, 0) &= \frac{R_m}{W_i}, \text{ for } 0 \leq k \leq W_i - 1 \\
 &\quad 1 \leq i \leq M + f
 \end{aligned} \tag{2}$$

TABLE II  
NOTATIONS USED IN THE ANALYSIS

Notation	Definition
$AC_m$	Four traffic flows with descending priorities (from 0 to 3)
$b(t)$	Backoff counter at time $t$
$s(t)$	Backoff stage at time $t$
$b_{i,k}$	Stationary probability of state $(s(t)=i, b(t)=k)$ in the first Markov chain
$CW_i$	Contention window size at backoff stage $i$
$L$	Average packet size
$l_i$	The number of slots in contention zone $i$
$M$	Maximum number of times the contention window may be increased
$M + f$	Frame retry limit
$p_i$	Probability that no station transmits in Zone $i$ in a slot time
$R_{mi}$	Collision probability of access category $m$ in Zone $i$
$P_{tr}[m]$	Probability of at least one transmission in a slot time for access category $m$
$Q_{mi}$	Probability of a successful transmission attempt in a slot for a specific access category $m$ in Zone $i$
$\Gamma_i$	Channel idle probability in Zone $i$
$S_m$	Average throughput of access category $m$
$t_i$	Stationary probability of state $i$ in the second Markov chain
$TS_m$	Average time the channel is sensed busy because of a successful transmission
$TC_m$	Average time the channel is sensed busy by each $AC_m$ during a collision
$T_H$	Transmission time periods of the frame header
$T_{SIFS}$	SIFS period
$T_{AIFS_m}$	AIFS period for access category $m$
$T_{ACK}$	ACK transmission time
$T_{L_m}$	Transmission time of the average payload of $AC_m$
$T_{L_m}^*$	Transmission time of the largest payload involved in a collision for access category $m$
$\delta$	Propagation delay
$\tau_m$	Transmission probability of $AC_m$
$Z_i$	Stationary distribution for Zone $i$

where  $M$  is the maximum number of times that the contention window (CW) may be increased,  $R_m$  is the collision probability, and  $M + f$  is the maximum number of trails before dropping a packet.  $(W_0 - 1)$  is the backoff window size at stage 0, which is equal to  $CW_{\min}$ .  $(W_i - 1)$  represents the backoff window size at stage  $i$ .

The first line in (2) accounts for the fact that the backoff counter is decreased by one at the beginning of each slot time. The second line in (2) corresponds to the case that the old frame has been successfully transmitted, and a new frame is about to be transmitted. Thus, the process randomly proceeds to one of the states in stage 0 when the transmission of a new frame starts, and the backoff counter is reset to a random value  $b(t)$  between 0 and  $(W_0 - 1)$ . The third line in (2) states that, once the backoff stage reaches the retry limit of  $M + f$ , the frame is discarded if the transmission is not successful. In this case, the next HOL data frame will be set for transmission. Thus, the process transits to one of the states in stage 0 with a probability

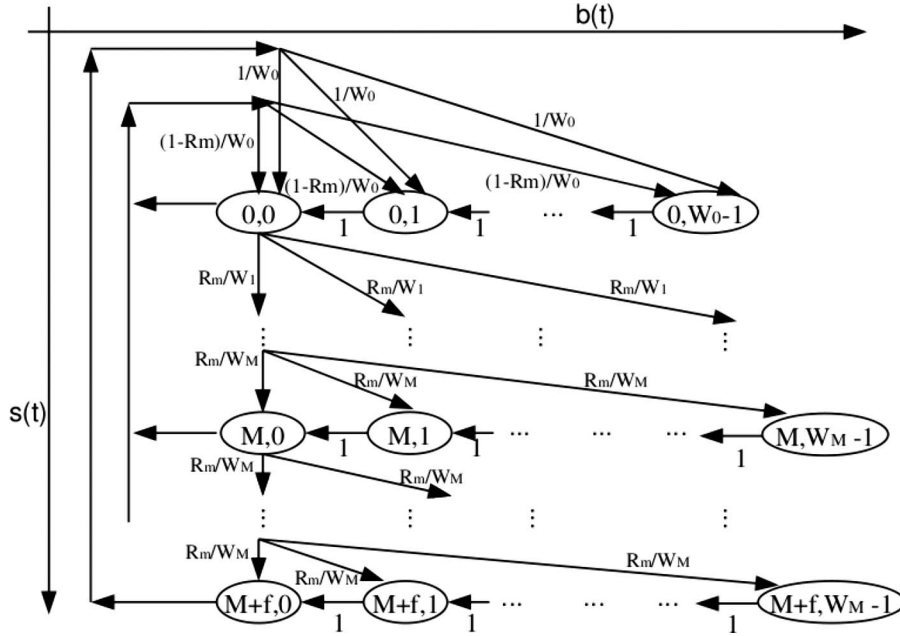


Fig. 3. Two-dimensional Markov chain for a single  $AC_m$ .

of 1. The last line in (2) describes the case of an unsuccessful transmission at backoff stage  $(i - 1)$ . In this case, the process moves to the next backoff stage, and the new backoff value is randomly chosen from interval  $[0, W_i - 1]$ . After stage  $M$ ,  $W_i$  is not increased beyond  $W_M = CW_{\max} + 1$ .

On the other hand, the maximum window size at stage  $i$ , i.e.,  $CW_i$ , is given by

$$CW_i = \begin{cases} CW_{\min}, & \text{for } i = 0 \\ 2 \cdot (CW_{i-1} + 1) - 1, & \text{for } 1 \leq i \leq M - 1 \\ CW_{\max}, & \text{for } M \leq i \leq M + f. \end{cases} \quad (3)$$

Thus

$$W_i = \begin{cases} CW_{\min} + 1, & \text{for } i = 0 \\ 2^i \cdot W_0, & \text{for } 1 \leq i \leq M - 1 \\ CW_{\max} + 1, & \text{for } M \leq i \leq M + f. \end{cases} \quad (4)$$

By solving the Markov chain in Fig. 3 as outlined in the Appendix, we can obtain a relation between  $\tau_m$  and  $R_m$ . The transmission probability  $\tau_m$  for  $AC_m$  queue in any given time slot can be obtained as follows:

$$\tau_m = \frac{2}{1 - R_m} \left( \frac{1}{1 - R_m} + W_0 \sum_{i=0}^M 2^i R_m^i + W_M \sum_{i=M+1}^{M+f} R_m^i \right)^{-1}. \quad (5)$$

Now, we need to find another equation that includes both  $\tau$  and  $R$  to compute the transmission probabilities for different ACs. In IEEE 802.11p, different ACs have different AIFS values, which are denoted by AIFS[AC]. In addition, the internal collisions inside each STA are treated by a scheduler inside that STA. To this end, the higher priority ACs have shorter AIFS values. Thus, as shown in Fig. 4, the contention period can be

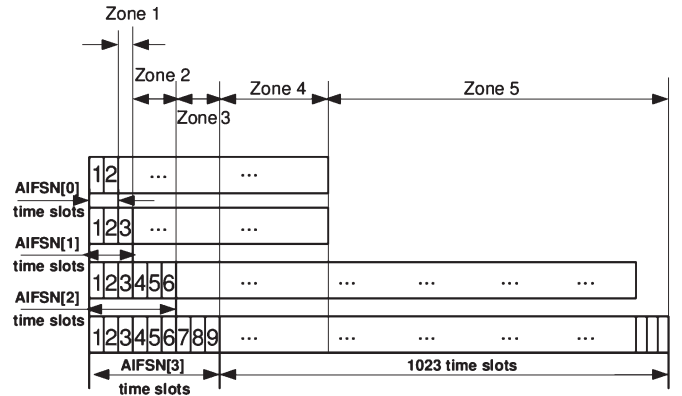


Fig. 4. Contention zones.

divided into different *contention zones*. According to the draft standard IEEE 802.11p [16], AIFS[0], AIFS[1], AIFS[2], and AIFS[3] last for two, three, six, and nine times the *SlotTime* duration, respectively. We know that collisions happen when more than one node or AC attempts to access the shared channel at the same time. Once the backoff timers in more than one EDCAF become zero, either an internal or an external collision happens. Internal collisions are resolved by a scheduler that grants the current TXOP to the AC queue with the highest priority. Thus, these collisions will not waste channel resources. Obviously, this is not the case for the external collisions as there is no prioritization mechanism for the stations. To this end, only external collisions could occur in Zone 1, i.e., from AC0 in different stations, whereas both external and internal collisions may occur in other zones. For example, in Zone 1, only AC0 traffic flows compete for the shared channel. In Zone 2, AC0 and AC1 traffic flows compete to access the channel. Accordingly, Zones 3, 4, and 5 will have increasing numbers of ACs competing for the shared channel, as shown in Fig. 4.

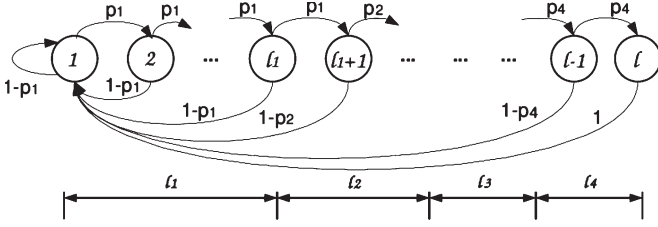


Fig. 5. Markov chain for slots in both contention zones.

However, under saturated conditions, there is no transmission chance in Zone 5 since, within Zones 1–4,  $AC_0$  and  $AC_1$  will try to transmit, after their short backoff timers. Note that, if the  $CW_{\max}$  of  $AC_0$  is 7 as in the IEEE 802.11p, under saturated traffic conditions,  $AC_3$  has no chance to transmit. Because  $CW_{0\max} + AIFS[0] = AIFS[3]$ , before  $AC_3$  finishes its AIFS defer, a station with  $AC_0$  starts a transmission. Hence, we change the maximum CWs of  $AC_0$  and  $AC_1$  to 15 and 14, respectively, to evaluate the performance of the four access categories of traffic. Meanwhile, since  $CW_{0\max} + AIFS[0] = CW_{1\max} + AIFS[1]$ , fewer zones need to be defined. Let  $l_i$  denote the number of time slots of Zone  $i$ ; thus, from Fig. 4

$$\begin{cases} l_1 = 1 \\ l_2 = 3 \\ l_3 = 3 \\ l_4 = 8 \\ l_5 = 1015. \end{cases} \quad (6)$$

We use a new discrete-time Markov chain to obtain the stationary probability of each contention zone, as shown in Fig. 5. State  $i$  in this Markov chain is visited if there has not been a successful access to the shared channel in time slots  $1, 2, \dots, i-1$ . There will be a transition from state  $i-1$  to  $i$  in time slot  $i$  if there is no attempt to transmit in time slot  $i-1$ . The probability of this event is different for different zones, as shown in Fig. 5.

The transition probabilities in the Markov chain in Fig. 5 are given in the following:

$$\begin{aligned} P(i+1|i) &= p_1, \text{ for } 1 \leq i \leq l_1 \\ P(i+1|i) &= p_2, \text{ for } l_1 + 1 \leq i \leq l_1 + l_2 \\ P(i+1|i) &= p_3, \text{ for } l_1 + l_2 + 1 \leq i \leq l_1 + l_2 + l_3 \\ P(i+1|i) &= p_4, \text{ for } l_1 + l_2 + l_3 + 1 \leq i \leq l-1 \\ P(1|i) &= 1 - p_1, \text{ for } 1 \leq i \leq l_1 \\ P(1|i) &= 1 - p_2, \text{ for } l_1 + 1 \leq i \leq l_1 + l_2 \\ P(1|i) &= 1 - p_3, \text{ for } l_1 + l_2 + 1 \leq i \leq l_1 + l_2 + l_3 \\ P(1|i) &= 1 - p_4, \text{ for } l_1 + l_2 + l_3 + 1 \leq i \leq l-1 \\ P(1|i) &= 1, \text{ for } i = l \end{aligned} \quad (7)$$

where  $l = l_1 + l_2 + l_3 + l_4$ .

Let us consider a network with  $N$  nodes, each with four saturated buffers for four different ACs. Denote by  $N_m$  the number of competing  $AC_m$  traffic flows. In a saturated scenario, we know that  $N_0 = N_1 = N_2 = N_3 = N$ , but we preserve different notations for the number of different competing ACs in the rest of the analysis for the sake of the generality of the proposed analysis. This will allow a simpler extension of the analysis for unsaturated scenarios. If the probability of transmission for  $AC_m$  is denoted by  $\tau_m$ , the transition probabilities in Fig. 5 can be calculated as follows:

$$\begin{cases} p_1 = (1 - \tau_0)^{N_0} \\ p_2 = (1 - \tau_0)^{N_0} (1 - \tau_1)^{N_1} \\ p_3 = (1 - \tau_0)^{N_0} (1 - \tau_1)^{N_1} (1 - \tau_2)^{N_2} \\ p_4 = (1 - \tau_0)^{N_0} (1 - \tau_1)^{N_1} (1 - \tau_2)^{N_2} (1 - \tau_3)^{N_3}. \end{cases} \quad (8)$$

Let  $t_i$  be the stationary probability of state  $i$  in the Markov chain of Fig. 5, which is defined as

$$t_i \triangleq \lim_{t \rightarrow \infty} P\{\text{State } i\}, \text{ for } 1 \leq i \leq l. \quad (9)$$

From the transition probabilities in (7)

$$t_{i+1} = \begin{cases} t_i \cdot p_1, & \text{for } 1 \leq i \leq l_1 \\ t_i \cdot p_2, & \text{for } l_1 + 1 \leq i \leq l_1 + l_2 \\ t_i \cdot p_3, & \text{for } l_1 + l_2 + 1 \leq i \leq l_1 + l_2 + l_3 \\ t_i \cdot p_4, & \text{for } l_1 + l_2 + l_3 + 1 \leq i \leq l-1. \end{cases} \quad (10)$$

Thus

$$t_i = \begin{cases} t_1 \cdot p_1^{i-1}, & \text{for } 1 \leq i \leq l_1 + 1 \\ t_1 \cdot p_1^{l_1} \cdot p_2^{i-l_1}, & \text{for } l_1 + 2 \leq i \leq l_1 + l_2 + 1 \\ t_1 \cdot p_1^{l_1} \cdot p_2^{l_2} \cdot p_3^{i-l_1-l_2-1}, & \text{for } l_1 + l_2 + 2 \leq i \leq l_1 + l_2 + l_3 + 1 \\ t_1 \cdot p_1^{l_1} \cdot p_2^{l_2} \cdot p_3^{l_3} \cdot p_4^{i-l_1-l_2-l_3-1}, & \text{for } l_1 + l_2 + l_3 + 2 \leq i \leq l. \end{cases} \quad (11)$$

Since the sum of all states in this Markov chain is equal to one

$$\begin{aligned} 1 &= \sum_{i=1}^l t_i = t_1 \\ &\cdot \left( \sum_{i=1}^{l_1+1} p_1^{i-1} + p_1^{l_1} \sum_{i=l_1+2}^{l_1+l_2+1} p_2^{i-l_1-1} \right. \\ &\quad + p_1^{l_1} p_2^{l_2} \sum_{i=l_1+l_2+2}^{l_1+l_2+l_3+1} p_3^{i-l_1-l_2-1} \\ &\quad \left. + p_1^{l_1} p_2^{l_2} p_3^{l_3} \sum_{i=l_1+l_2+l_3+2}^l p_4^{i-l_1-l_2-l_3-1} \right) \\ &= t_1 \left( \frac{1 - p_1^{l_1+1}}{1 - p_1} + p_1^{l_1} p_2 \frac{1 - p_2^{l_2}}{1 - p_2} + p_1^{l_1} p_2^{l_2} p_3 \frac{1 - p_3^{l_3}}{1 - p_3} \right. \\ &\quad \left. + p_1^{l_1} p_2^{l_2} p_3^{l_3} p_4 \frac{1 - p_4^{l-l_1-l_2-l_3-1}}{1 - p_4} \right). \end{aligned} \quad (12)$$

Hence

$$t_1 = \left( \frac{1 - p_1^{l_1+1}}{1 - p_1} + p_1^{l_1} p_2 \frac{1 - p_2^{l_2}}{1 - p_2} + p_1^{l_1} p_2^{l_2} p_3 \frac{1 - p_3^{l_3}}{1 - p_3} + p_1^{l_1} p_2^{l_2} p_3^{l_3} p_4 \frac{1 - p_4^{l_4-1}}{1 - p_4} \right)^{-1}. \quad (13)$$

Therefore, the stationary probability of Zone  $i$ , which is denoted by  $Z_i$ , is given by

$$\begin{cases} Z_1 = \sum_{i=1}^{l_1} t_i \\ Z_2 = \sum_{i=l_1+1}^{l_1+l_2} t_i \\ Z_3 = \sum_{i=l_1+l_2+1}^{l_1+l_2+l_3} t_i \\ Z_4 = \sum_{i=l_1+l_2+l_3+1}^l t_i. \end{cases} \quad (14)$$

Now, we can calculate the collision probability experienced by each AC as follows: Let  $R_{mi}$  be the probability of collision for AC  $m$  in Zone  $i$ . Hence

$$\begin{cases} R_0 = \frac{Z_1 R_{01} + Z_2 R_{02} + Z_3 R_{03} + Z_4 R_{04}}{Z_1 + Z_2 + Z_3 + Z_4} \\ R_1 = \frac{Z_2 R_{12} + Z_3 R_{13} + Z_4 R_{14}}{Z_2 + Z_3 + Z_4} \\ R_2 = \frac{Z_3 R_{23} + Z_4 R_{24}}{Z_3 + Z_4} \\ R_3 = R_{34}. \end{cases} \quad (15)$$

According to Fig. 4,  $R_{mi}$  ( $m = 0, 1, 2, 3$  and  $i = 1, 2, 3, 4$ ) can be calculated as follows:

$$\begin{aligned} R_{01} &= 1 - (1 - \tau_0)^{N_0-1} \\ R_{02} &= 1 - (1 - \tau_0)^{N_0-1} (1 - \tau_1)^{N_1-1} \\ R_{03} &= 1 - (1 - \tau_0)^{N_0-1} (1 - \tau_1)^{N_1-1} (1 - \tau_2)^{N_2-1} \\ R_{04} &= 1 - (1 - \tau_0)^{N_0-1} (1 - \tau_1)^{N_1-1} (1 - \tau_2)^{N_2-1} (1 - \tau_3)^{N_3-1} \\ R_{12} &= 1 - (1 - \tau_0)^{N_0} (1 - \tau_1)^{N_1-1} \\ R_{13} &= 1 - (1 - \tau_0)^{N_0} (1 - \tau_1)^{N_1-1} (1 - \tau_2)^{N_2-1} \\ R_{14} &= 1 - (1 - \tau_0)^{N_0} (1 - \tau_1)^{N_1-1} (1 - \tau_2)^{N_2-1} (1 - \tau_3)^{N_3-1} \\ R_{23} &= 1 - (1 - \tau_0)^{N_0} (1 - \tau_1)^{N_1} (1 - \tau_2)^{N_2-1} \\ R_{24} &= 1 - (1 - \tau_0)^{N_0} (1 - \tau_1)^{N_1} (1 - \tau_2)^{N_2-1} (1 - \tau_3)^{N_3-1} \\ R_{34} &= 1 - (1 - \tau_0)^{N_0} (1 - \tau_1)^{N_1} (1 - \tau_2)^{N_2} (1 - \tau_3)^{N_3-1} \\ R_{11} &= R_{21} = R_{22} = R_{31} = R_{32} = R_{33} = 0. \end{aligned} \quad (16)$$

Now, we can solve the equation set (5) for each AC and (15) and (16) to obtain transmission probabilities and collision probabilities for different ACs. Then, these quantities can be used to obtain throughput for each AC.

Before the calculation of the normalized throughput for each AC, we define some probabilities to be used in the latter part. Let  $P_{tr}[m]$  be the probability that at least there is one transmission attempt from AC  $m$  in a given time slot. Denote

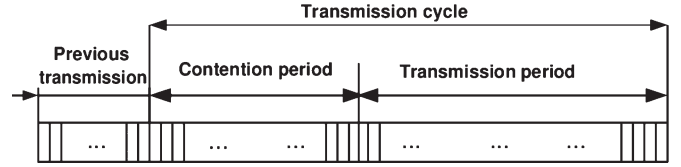


Fig. 6. Consistency of the transmission cycle duration.

by  $Q_{mi}$  the probability of successful transmission for AC  $m$  in Zone  $i$

$$P_{tr}[i] = 1 - (1 - \tau_i)^{N_i}, \text{ for } 0 \leq i \leq 3. \quad (17)$$

In addition, the probability of successful transmission for AC  $m$  in Zone  $i$ , for  $m = 0, 1, 2, 3$  and  $i = 1, 2, 3, 4$ , can be calculated as follows:

$$\begin{cases} Q_{01} = \frac{N_0 \tau_0 (1 - \tau_0)^{N_0-1}}{P_{tr}[0]} \\ Q_{02} = Q_{01} \cdot (1 - \tau_1)^{N_1-1} \\ Q_{03} = Q_{02} \cdot (1 - \tau_2)^{N_2-1} \\ Q_{04} = Q_{03} \cdot (1 - \tau_3)^{N_3-1} \\ Q_{12} = \frac{N_1 \tau_1 (1 - \tau_0)^{N_0} (1 - \tau_1)^{N_1-1}}{P_{tr}[1]} \\ Q_{13} = Q_{12} \cdot (1 - \tau_2)^{N_2-1} \\ Q_{14} = Q_{13} \cdot (1 - \tau_3)^{N_3-1} \\ Q_{23} = \frac{N_2 \tau_2 (1 - \tau_0)^{N_0} (1 - \tau_1)^{N_1} (1 - \tau_2)^{N_2-1}}{P_{tr}[2]} \\ Q_{24} = Q_{23} \cdot (1 - \tau_3)^{N_3-1} \\ Q_{34} = \frac{N_3 \tau_3 (1 - \tau_0)^{N_0} (1 - \tau_1)^{N_1} (1 - \tau_2)^{N_2} (1 - \tau_3)^{N_3-1}}{P_{tr}[3]} \\ Q_{11} = Q_{21} = Q_{22} = Q_{31} = Q_{32} = Q_{33} = 0. \end{cases} \quad (18)$$

The channel idle probability for a slot in each zone can be calculated by

$$\begin{cases} \Gamma_1 = (1 - \tau_0)^{N_0} \\ \Gamma_2 = \prod_{i=0}^1 (1 - \tau_i)^{N_i} \\ \Gamma_3 = \prod_{i=0}^2 (1 - \tau_i)^{N_i} \\ \Gamma_4 = \prod_{i=0}^3 (1 - \tau_i)^{N_i}. \end{cases} \quad (19)$$

Thus, the throughput of AC  $m$ , which is denoted by  $S_m$ , is defined as the fraction of time from a transmission cycle used for successful transmission of bits for AC  $m$ .  $S_m$  is given by

$$S_m = \frac{\sum_{i=0}^5 Z_i P_{tr}[m] Q_{mi} E[L]}{\text{average length of a transmission cycle}}. \quad (20)$$

A transmission cycle consists of the contention period and the transmission period, as shown in Fig. 6. During the contention period, nodes start their own backoff procedure after the channel is sensed idle for its own AIFS; in RTS/CTS mode, the contention period we defined here includes channel negotiation. The transmission period begins after all the sensing, backoff, and channel negotiations are finished, and nodes start to transmit data over the channel. Thus, the denominator of (20) is given by

$$\begin{aligned} &\text{average length of tran. cycle} \\ &= E[\text{contention period}] + E[\text{transmission period}]. \end{aligned} \quad (21)$$

As mentioned earlier

contention period

$$= \text{AIFS} + \text{backoff timer} + \text{channel negotiation} \quad (22)$$

where the backoff time is separately calculated, whereas the time costs on AIFS and channel negotiation are calculated together with the transmission period. Thus, (21) is rewritten as

$$\begin{aligned} \text{average length of tran. cycle} &= E[\text{duration of idle slots}] \\ &+ E[\text{duration of transmission slots}]. \quad (23) \end{aligned}$$

To calculate the length of a transmission cycle, first, we analyze all possible events for each slot similarly, as mentioned in [18]. Three types of events could happen in a slot: 1) idle, where there is no transmission; 2) transmission, where there is only one transmission; and 3) collision, where there is more than one simultaneous transmission. In Zone  $i$ , the probability of having an idle slot is denoted by  $\Gamma_i$ , as calculated in (19), and the probability of transmission in a time slot is given by

$$\sum_{m=0}^3 P_{\text{tr}}[m]Q_{mi}.$$

The probability of collision in a time slot is given by

$$1 - \Gamma_i - \sum_{m=0}^3 P_{\text{tr}}[m]Q_{mi}.$$

Considering the state in the backoff procedure from which a transmission starts, we can obtain an average number of idle slots in each zone. For example, if the special state is in Zone 2, its backoff timer could be at one of slots 2–4, which means that the number of idle slots could be 1, 2, or 3. Thus, the average length of idle slots provided that the state is in Zone 2 is given by  $Z_2(1 \times \Gamma_2 + 2 \times \Gamma_2^2 + 3 \times \Gamma_2^3) \times \text{SlotTime}$ . Hence

$$\begin{aligned} &E[\text{duration of backoff slots in a cycle}] \\ &= \left( Z_1\Gamma_1 \times 0 + Z_2 \sum_{t=1}^{l_2} (t + l_1 - 1)\Gamma_2^t \right. \\ &\quad + Z_3 \sum_{t=1}^{l_3} (t + l_2 + l_1 - 1)\Gamma_3^t \\ &\quad \left. + Z_4 \sum_{t=1}^{l_4} (t + l_3 + l_2 + l_1 - 1)\Gamma_4^t \right) \times \text{SlotTime}. \quad (24) \end{aligned}$$

$E[\text{transmission slots}]$

$$\begin{aligned} &= \sum_{i=1}^4 Z_i \sum_{m=0}^3 P_{\text{tr}}[m]Q_{mi}TS_m \\ &+ \left( 1 - \sum_{i=1}^4 Z_i\Gamma_i - \sum_{i=1}^4 Z_i \sum_{m=0}^3 P_{\text{tr}}[m]Q_{mi} \right) TC_0 \quad (25) \end{aligned}$$

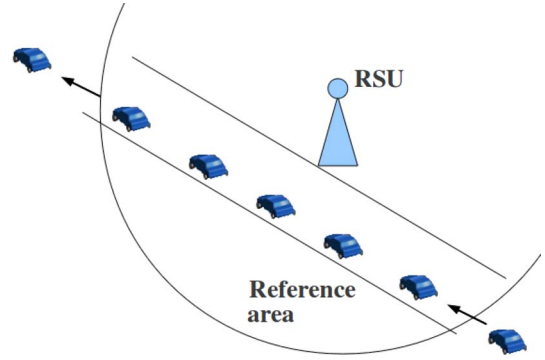


Fig. 7. Simulation scenario.

where  $TS_m$  is the average time in which the channel is sensed busy because of a successful transmission of  $AC_m$ , and  $TC_m$  is the average time in which the channel is sensed busy by  $AC_m$ , whereas  $TC^*$  is the minimum of  $TC_m$ , which are involved in the collisions. The expressions  $TS_m$  and  $TC_m$  for  $AC_m$  in the basic access mode can be derived as follows:

$$\begin{aligned} TS_m &= T_{\text{AIFS}[m]} + T_H + T_{L_m} + \delta + T_{\text{SIFS}} + T_{\text{ACK}} + \delta \\ TC_m &= T_{\text{AIFS}[m]} + T_H + T_{L_m^*} + \delta \quad (26) \end{aligned}$$

where  $T_H$  is the transmission time periods of the frame header, and  $T_{\text{SIFS}}$  and  $T_{\text{AIFS}[m]}$  are the SIFS and AIFS periods, respectively.  $T_{\text{ACK}}$  is the ACK transmission time,  $T_{L_m}$  is the transmission time of the average payload,  $T_{L_m^*}$  is the transmission time of the largest payload involved in a collision, and  $\delta$  is the propagation delay. For the RTS/CTS access mode

$$\begin{aligned} TS_m &= T_{\text{AIFS}[m]} + T_{\text{RTS}} + \delta + T_{\text{SIFS}} + T_{\text{CTS}} + \delta \\ &\quad + T_{\text{SIFS}} + T_H + T_{L_m} + \delta + T_{\text{SIFS}} + T_{\text{ACK}} + \delta \\ TC_m &= T_{\text{AIFS}[m]} + T_{\text{RTS}} + \delta. \quad (27) \end{aligned}$$

Thus, from the set of (20) and (23)–(25), the average throughput for each AC can be derived. As it can be seen from the final expression, although RTS/CTS assists to avoid the hidden terminal problem, the overhead caused by the acknowledgment and handshakes reduces the performance of systems with high mobility, such as vehicular networks. The RTS/CTS access mode exhibits superior efficiency in relatively low velocity, whereas the basic access mode performs better, in terms of throughput, than RTS/CTS in high velocities [19] (see Fig. 7).

## V. SIMULATION RESULTS

In this section, first, we present simulation results to validate the accuracy of the proposed analytical model. Then, the performance of the service differentiation capability of the IEEE 802.11p, in terms of throughput and queuing delay, is analyzed and compared to that of 802.11 and 802.11e. Finally, the impact of a large number of nodes on the performance the IEEE 802.11p is investigated.

TABLE III  
PARAMETER SETTING

Packet payload	512 bytes, 1000 bytes
Data rate	6, 11 Mbps
Slot time	13 $\mu$ s
SIFS	32 $\mu$ s
DIFS	58 $\mu$ s
$\delta$	2 $\mu$ s
AC0 $CW_{min}$	3 time slots
AC0 $CW_{max}$	15 time slots
AC1 $CW_{min}$	3 time slots
AC1 $CW_{max}$	14 time slots
AC2 $CW_{min}$	15 time slots
AC2 $CW_{max}$	1023 time slots
AC3 $CW_{min}$	15 time slots
AC3 $CW_{max}$	1023 time slots

We use the well-known simulation tool NS-2 [20] from Lawrence Berkeley National Laboratory and the implementation of 802.11e EDCA [22] in NS-2 from the TKN group in the Technical University of Berlin. Some parts of the original simulation codes have been changed according to the draft standard IEEE 802.11p [16] in our work, such as the AIFS and CW parameters. In addition, we fix the bugs of the RTS/CTS mode to make successful transmission using the RTS/CTS mechanism. We use this model to analyze the performance of the MAC sublayer in saturated scenarios. We also amend our results by simulation-based performance analysis for nonsaturated cases. The reference area is a circular area around the roadside unit (RSU), with a radius that is equal to the transmission range. Vehicles enter the reference area of the RSU in equal intervals, which means the distance between two adjacent vehicles is fixed in each scenario. The number of vehicles in the reference area is controlled by changing the distance among vehicles. When a vehicle enters the communication range of the RSU, it initiates constant-bit-rate data transmission to the RSU. The stations contend to transmit fixed-size UDP packets to the RSU. Handoff is not considered in such scenarios at the current stage. The speed of the vehicles is set to be 70 mi/h, according to the typical speed limit for motorways. In [21], the commonly assumed default 6-Mb/s data rate is justified to be the best selection for various intended ranges and safety message sizes in most cases. As a result, in our simulations, the data rate is set to 6 Mb/s. We compare the system performance in terms of throughput using different data rates (i.e., 11 and 6 Mb/s). The rest of the major simulation parameters are chosen from the latest draft IEEE 802.11p standard, as listed in Table III.

#### A. Validation of the Analytical Model

In this section, we consider a scenario where one RSU is placed at the middle of the reference area, surrounded by different numbers of vehicles traveling in a circular track around the RSU in each simulation. The simulations in this section are implemented in such a scenario that allows the system to

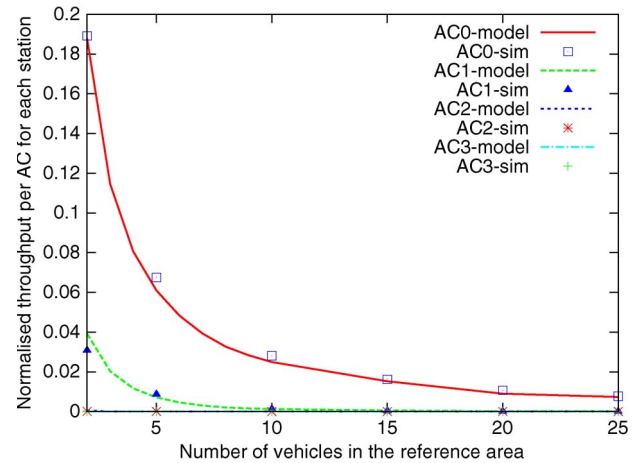


Fig. 8. Normalized average throughput per AC for each station versus the number of vehicles in the reference area.

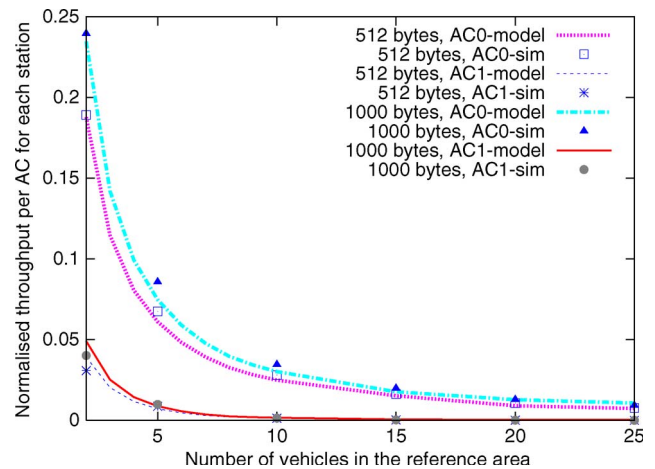


Fig. 9. Impact of packet size on system performance in terms of throughput.

achieve steady performance, disregarding the effects from fast vehicle movements. Each node is equipped with four ACs. The interval of packet arrival is 1 ms, such that each AC queue is assumed to be saturated.

Fig. 8 shows the analytical and simulation results for the normalized average throughput per AC for each station versus the number of vehicles in the reference area. The first observation in Fig. 8 is that the results from the analytical model match those of the simulations. The normalized measured throughput is calculated by dividing the nonnormalized throughput by the channel capacity. As the number of vehicles increases, the throughput for each station quickly decreases due to the increasing collisions among the stations. AC0 enjoys the highest throughput, compared with other ACs. AC2 and AC3 seldom have the chance to transmit over the channel because of the saturated scenario in this simulation.

In the second set of simulations, the packet size is increased to 1000 B. Comparing with the results from simulations in which the packet size is 512 B, throughput is higher when the packet size is larger, as shown in Fig. 9. It costs the same time on the channel negotiation; thus, the larger the packet size, the higher the throughput that will be achieved.

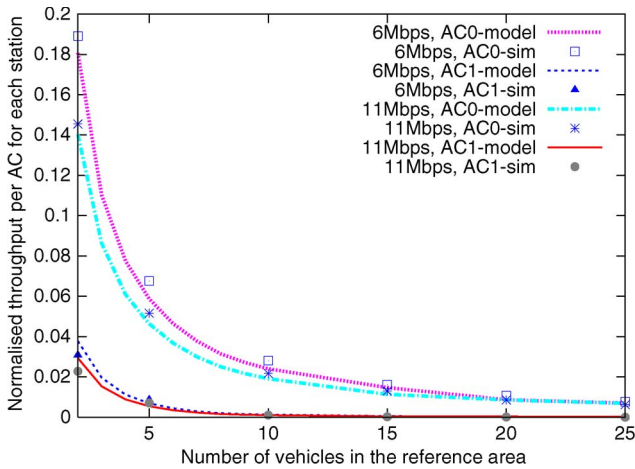


Fig. 10. Impact of channel data rate on system performance in terms of throughput.

TABLE IV  
DESCRIPTION OF TRAFFIC FLOWS

	VoIP	Video	Best effort	Background
AC	AC_VO(0)	AC_VI(1)	AC_BE(2)	AC_BK(3)
Packet size	160 bytes	256 bytes	200 bytes	200 bytes
Data rate	64 kb/s	64 kb/s	128 kb/s	256 kb/s
Interval	20 ms	32 ms	12.5 ms	6.25 ms

Another comparison is made using the same packet size (i.e., 512 B) but different channel data rates. Fig. 10 shows the normalized average throughput per AC for each station versus the number of vehicles in the reference area. The nonnormalized aggregate throughput is higher using a higher channel data rate, whereas the normalized throughput is higher using 6-Mb/s data rate. Although the higher data rate channel costs less time for data transmission, the time consumed in the backoff procedure is the same as that in lower data rate channel.

B. Comparison of 802.11p With 802.11 and 802.11e

In this section, first, we compare the service differentiation capabilities of the IEEE 802.11p with its predecessors, i.e., 802.11 and 802.11e, in terms of per-AC throughput and queuing delays. Then, we provide the overall system-level throughput for IEEE 802.11p. The generic setting up of the scenario is the same as the description at the beginning of this section.

1) Service Differentiation: To observe the differentiation of service in 802.11p, the simulation scenario is designed as follows: Each vehicle is able to transmit four different categories of traffic flows (i.e., AC\_VO, AC\_VI, AC\_BE, and AC\_BK), which are defined in the draft standard of IEEE 802.11p. Every 5 s, each vehicle randomly switches its traffic category. The four traffic categories are given as follows: 1) high-priority audio flow (64 kb/s); 2) H.263 video flow (64 kb/s) with medium priority; 3) best effort with low priority; and 4) background traffic with the lowest priority. The different traffic flows are described in Table IV. The rest of the simulation parameters are the same as specified in the beginning of Section V.

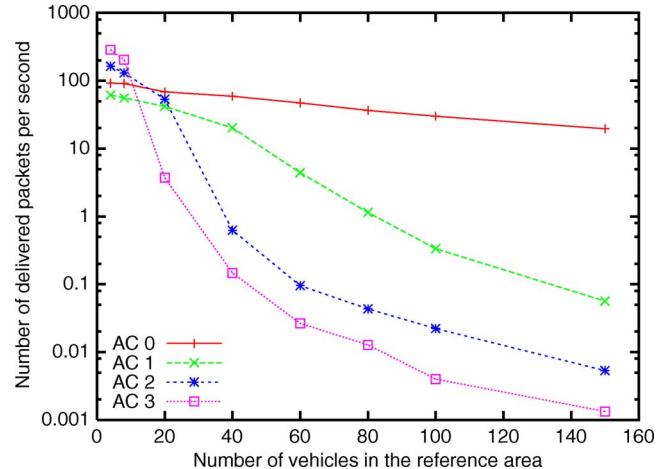


Fig. 11. Numbers of delivered packets per second of each AC with IEEE 802.11p.

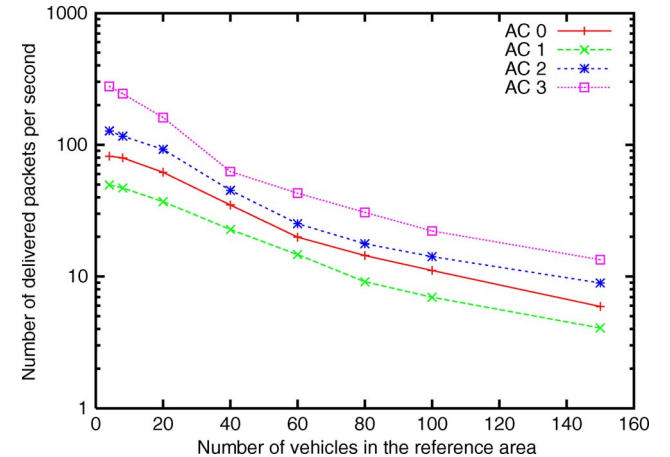


Fig. 12. Numbers of delivered packets per second of each AC with IEEE 802.11p.

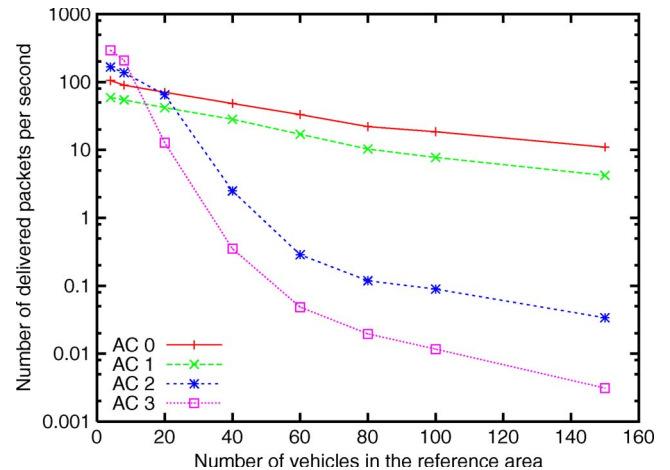


Fig. 13. Numbers of delivered packets per second of each AC with IEEE 802.11e.

Figs. 11–13 show the number of delivered packets per second of each AC in different systems in the log-scaled coordinate systems. As 802.11 does not provide service differentiation

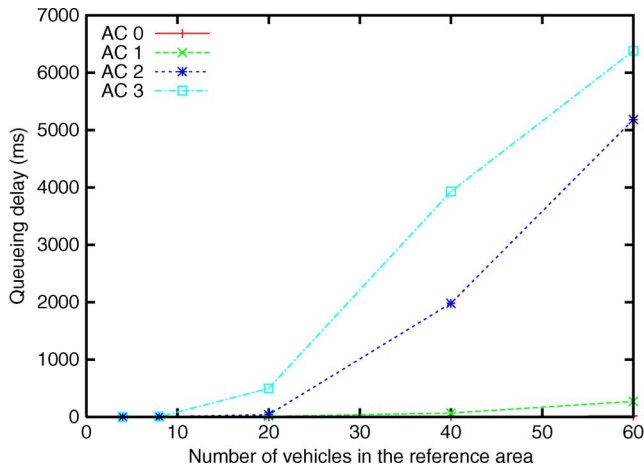


Fig. 14. Queuing delay for each AC in the IEEE 802.11p system.

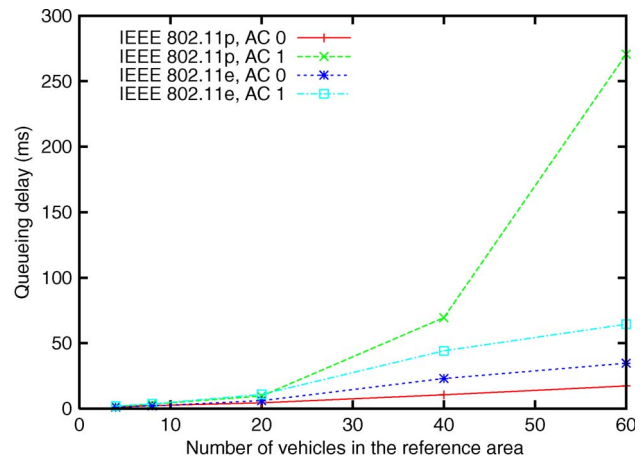


Fig. 15. Queuing delays for higher priority ACs in IEEE 802.11e/p systems.

support, different ACs compete for the transmission opportunities with equal priority. For 802.11p, when the number of active stations in the reference area is low, contentions among stations are not severe. Hence, due to the large packet size and short interval, the lower priority traffic flows do not significantly suffer. However, as the number of competing stations increases, traffic flows with higher priorities enjoy significantly more chances of transmission. For the two higher priority traffic flows, the highest priority traffic flow has absolute advantage over the lower priority traffic flow. Due to the modification of parameters from IEEE 802.11e, in IEEE 802.11p, the traffic flows with the highest priority is highly protected and granted most of the system throughput. While in 802.11e, differentiation between these two categories of traffic flows is not so obvious. From Fig. 13, in IEEE 802.11e, traffic flows with two higher priorities occupy the channel mostly when the number of stations is high. Traffic flows with lower priorities seldom have opportunities to transmit via the channel in both 802.11e and 802.11p systems. IEEE 802.11p provides better service differentiation than 802.11e.

Fig. 14 shows the queuing delay for each AC as the number of stations in the reference area varies. For the two higher priority ACs, the queuing delays remain at a low level (e.g., 17.3 and 270 ms for AC0 and AC1, respectively, with 60 stations in contention), whereas the queuing delays for the other two ACs with lower priorities increase fast. Services with high priority have neglectable queuing delays to fulfil the requirements of delay in ITS safety-related applications and traffic management applications. AC2 and AC3 are suitable for nontime-critical ITS applications that do not have strict requirement on delay parameters, such as web surfing, emails, travel information collection, and database updates.

Fig. 15 compares queuing delays for two higher priority ACs in different systems as the number of stations in the reference area varies. From the simulation results, the queuing delay for the highest priority AC is lower than AC1 in both cases. In IEEE 802.11e, AC0 and AC1 have the same AIFSs, so the prioritized service is provided by different CW sizes. In IEEE 802.11p, not only are the CW sizes different but the AIFS of AC1 is also larger; thus, the queuing delay of AC1

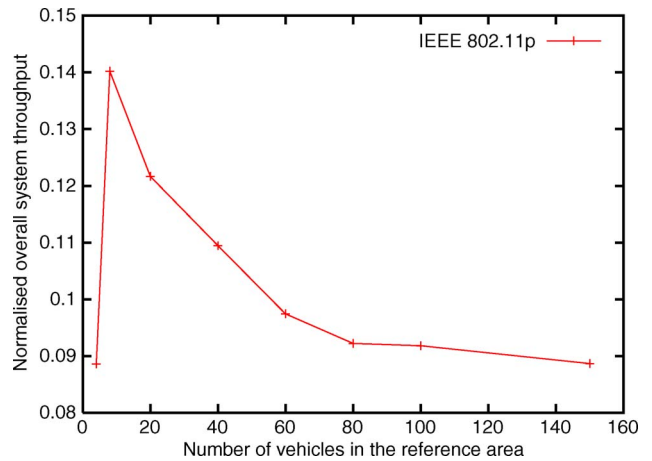


Fig. 16. Normalized overall system throughput as the number of stations varies.

in 802.11p is much larger than the rest of the AC queues in the figure.

2) *Overall System Throughput:* The normalized overall system throughput depends on the number of vehicles in the reference area. Fig. 16 shows the comparison of the overall system throughput for 802.11p. It can be seen that the overall system throughput rapidly increases as the number of the station increases. However, after a certain number of users, the overall system throughput declines due to the increasing level of contention in the system.

In vehicular networks, dense networks often form in urban areas or by traffic jams in intersections, accidents, and etc. In these scenarios, hundreds or even thousands of vehicles may exist in the same reference area, which could overload the shared wireless medium. Simulation results indicate that, as the number of stations in the reference area increases, the throughput of the system reduces after it reaches the maximum value. Alternative algorithms that adopt the principle of cluster [38] or multiple channels [39] should be considered to deal with the problem raised by the high node density in vehicular communication environments.

## VI. CONCLUSION

An analytical model for the performance of analysis of the IEEE 802.11p MAC sublayer has been proposed and evaluated by comprehensive simulations in this paper, which helps researchers to be confident about the accuracy of simulators and proceed to do further research on IEEE 802.11p. Our analysis has indicated that 802.11p provides effective service differentiation mechanism that can be suitable for mission-critical ITS applications. This stems from an enhanced and customized MAC sublayer design for the 802.11p standard. Nonetheless, supporting more bandwidth-consuming applications in 802.11p still remains as a challenging resource allocation problem. In addition, 802.11p demonstrates poor performance in highly populated and dense networks with too many stations.

### APPENDIX

#### RELATION BETWEEN $\tau_m$ AND $R_m$

We analyze the Markov chain in Fig. 3 to obtain the transmission probability for the  $AC_m$  queue in any given time slot. Let  $b_{i,k}$  be the stationary probability of state  $[s(t) = i, b(t) = k]$  in the Markov chain, i.e.,

$$b_{i,k} \triangleq \lim_{t \rightarrow \infty} P[s(t) = i, b(t) = k]$$

for  $0 \leq i \leq M + f, 0 \leq k \leq W_i - 1$ . (28)

From the transition probabilities in (2), the process will transit from  $[i, k + 1]$  to  $[i, k]$  with a probability of 1. Hence

$$\begin{cases} b_{0,0} = b_{0,1} + \frac{1}{W_0} \cdot \left( (1 - R_m) \sum_{i=0}^{M+f-1} b_{i,0} + b_{M+f,0} \right) \\ b_{0,1} = b_{0,2} + \frac{1}{W_0} \cdot \left( (1 - R_m) \sum_{i=0}^{M+f-1} b_{i,0} + b_{M+f,0} \right) \\ \vdots \\ b_{0,W_0-1} = \frac{1}{W_0} \cdot \left( (1 - R_m) \sum_{i=0}^{M+f-1} b_{i,0} + b_{M+f,0} \right). \end{cases} \quad (29)$$

Thus, for any state at stage 0

$$b_{0,k} = \frac{W_0 - k}{W_0} \cdot b_{0,0}. \quad (30)$$

For any state on the other nonzero stages

$$\begin{cases} b_{i,0} = b_{i,1} + b_{i-1,0} \cdot \frac{R_m}{W_i} \\ b_{i,1} = b_{i,2} + b_{i-1,0} \cdot \frac{R_m}{W_i} \\ \vdots \\ b_{i,W_i-1} = b_{i-1,0} \cdot \frac{R_m}{W_i}. \end{cases} \quad (31)$$

Thus

$$b_{i-1,0} \cdot R_m = b_{i,0}, \text{ for } 1 \leq i \leq M + f. \quad (32)$$

Hence

$$b_{i,0} = (R_m)^i \cdot b_{0,0}, \text{ for } 0 \leq i \leq M + f. \quad (33)$$

We could obtain the relationship between  $b_{i,k}$  and  $b_{i,0}$  from (31) as follows: For any state at other nonzero stages

$$b_{i,k} = \frac{W_i - k}{W_i} \cdot R_m \cdot b_{i-1,0}$$

for  $1 \leq i \leq M + f, 0 \leq k \leq W_i - 1$ . (34)

From (32), we could rewrite (34) as

$$b_{i,k} = \frac{W_i - k}{W_i} \cdot b_{i,0}. \quad (35)$$

Thus, for  $0 \leq k \leq W_i - 1$

$$b_{i,k} = \frac{W_i - k}{W_i} \cdot b_{i,0}, \text{ for } 0 \leq i \leq M + f. \quad (36)$$

Since the sum of all states in the Markov chain is equal to one

$$\begin{aligned} 1 &= \sum_{i=0}^{M+f} \sum_{k=0}^{W_i-1} b_{i,k} = \sum_{i=0}^{M+f} b_{i,0} \sum_{k=0}^{W_i-1} \frac{W_i - k}{W_i} \\ &= \sum_{i=0}^{M+f} b_{i,0} \frac{W_i + 1}{2} = \frac{b_{0,0}}{2} \sum_{i=0}^{M+f} R_m^i (W_i + 1) \\ &= \frac{b_{0,0}}{2} \left( \frac{1}{1 - R_m} + W_0 \sum_{i=0}^M 2^i R_m^i + W_M \sum_{i=M+1}^{M+f} R_m^i \right). \end{aligned} \quad (37)$$

Hence

$$b_{0,0} = 2 \left( \frac{1}{1 - R_m} + W_0 \sum_{i=0}^M 2^i R_m^i + W_M \sum_{i=M+1}^{M+f} R_m^i \right)^{-1}. \quad (38)$$

Since a transmission occurs whenever the backoff counter becomes zero, the transmission probability for an AC can be expressed by

$$\tau_m = \sum_{i=0}^{M+f} b_{i,0} = b_{0,0} \sum_{i=0}^{M+f} (R_m)^i = \frac{b_{0,0}}{1 - R_m}. \quad (39)$$

Replacing  $b_{0,0}$  from (38) in (39), the probability of transmission, i.e.,  $\tau_m$ , can be obtained as follows:

$$\tau_m = \frac{2}{1 - R_m} \left( \frac{1}{1 - R_m} + W_0 \sum_{i=0}^M 2^i R_m^i + W_M \sum_{i=M+1}^{M+f} R_m^i \right)^{-1}. \quad (40)$$

## ACKNOWLEDGMENT

This work was carried out within DRIVE C2X project which is funded by the European Union's Seventh Framework Programme (FP7/2007-2013) under Grant Agreement 270410.

## REFERENCES

- [1] DRIVE C2X Project. [Online]. Available: <http://www.drivec2x.eu/project>
- [2] F.-Y. Wang, "Parallel control and management for intelligent transportation systems: Concepts, architectures, and applications," *IEEE Trans. Intell. Transp. Syst.*, vol. 11, no. 3, pp. 630–638, Sep. 2010.
- [3] L. Figueiredo, I. Jesus, J. Machado, J. Ferreira, and J. Martins de Carvalho, "Towards the development of intelligent transportation systems," in *Proc. IEEE Intell. Transp. Syst.*, 2001, pp. 1206–1211.
- [4] M. Sichertiu and M. Kihl, "Inter-vehicle communication systems: A survey," *IEEE Commun. Surveys Tuts.*, vol. 10, no. 2, pp. 88–105, 2nd Quarter 2008.
- [5] R. Lu, X. Lin, H. Zhu, and X. Shen, "SPARK: A new VANET-based smart parking scheme for large parking lots," in *Proc. IEEE INFOCOM*, Apr. 19–25, 2009, pp. 1413–1421.
- [6] D. Greene, J. Liu, J. Reich, Y. Hirokawa, A. Shinagawa, H. Ito, and T. Mikami, "An efficient computational architecture for a collision early-warning system for vehicles, pedestrians, and bicyclists," *IEEE Trans. Intell. Transp. Syst.*, vol. 12, no. 4, pp. 942–953, Dec. 2011.
- [7] W.-Y. Shieh, C.-C. Hsu, S.-L. Tung, P.-W. Lu, T.-H. Wang, and S.-L. Chang, "Design of infrared electronic-toll-collection systems with extended communication areas and performance of data transmission," *IEEE Trans. Intell. Transp. Syst.*, vol. 12, no. 1, pp. 25–35, Mar. 2011.
- [8] Y. Bi, L. X. Cai, X. Shen, and H. Zhao, "Efficient and reliable broadcast in inter-vehicle communications networks: A cross layer approach," *IEEE Trans. Veh. Technol.*, vol. 59, no. 5, pp. 2404–2417, Jun. 2010.
- [9] A. Abdrabou and W. Zhuang, "Probabilistic delay control and road side unit placement for vehicular ad hoc networks with disrupted connectivity," *IEEE J. Sel. Areas Commun.*, vol. 29, no. 1, pp. 129–139, Jan. 2011.
- [10] H. T. Cheng, H. Shan, and W. Zhuang, "Infotainment and road safety service support in vehicular networking: From a communication perspective," *Mech. Syst. Signal Process., Special Issue Integr. Veh. Dyn.*, vol. 25, no. 6, pp. 2020–2038, Aug. 2011.
- [11] B. Gukhool and S. Cherkaoui, "IEEE 802.11p modeling in NS-2," in *Proc. 33rd IEEE Conf. LCN*, 2008, pp. 622–626.
- [12] S. Eichler, "Performance evaluation of the IEEE 802.11p WAVE communication standard," in *Proc. IEEE 66th VTC-2007 Fall*, 2007, pp. 2199–2203.
- [13] T. Murray, M. Cojocari, and H. Fu, "Measuring the performance of IEEE 802.11p using ns-2 simulator for vehicular networks," in *Proc. IEEE Int. Conf. EIT*, 2008, pp. 498–503.
- [14] *Wireless LAN Medium Access Control (MAC) and Physical Layer (PHY) Specifications*, IEEE Std. 802.11, Jun. 2007.
- [15] *Wireless LAN Medium Access Control (MAC) and Physical Layer (PHY) specifications Amendment 8: Medium Access Control (MAC) Quality of Service Enhancements*, IEEE Std. 802.11e, Nov. 2005.
- [16] *Wireless LAN Medium Access Control (MAC) and Physical Layer (PHY) specifications Amendment 7: Wireless Access in Vehicular Environments*, IEEE Unapproved Draft Std. P802.11p/D8.0, Jul. 2009.
- [17] L. Cheng, B. Henty, R. Cooper, D. Stancil, and F. Bai, "A measurement study of time-scaled 802.11a waveforms over the mobile-to-mobile vehicular channel at 5.9 GHz," *IEEE Commun. Mag.*, vol. 46, no. 5, pp. 84–91, May 2008.
- [18] G. Bianchi, "Performance analysis of the IEEE 802.11 distributed coordination function," *IEEE J. Sel. Areas Commun.*, vol. 18, no. 3, pp. 535–547, Mar. 2000.
- [19] S. D. Jung, S. W. Park, and S. S. Lee, "Effect of MAC throughputs according to relative velocity in vehicle ad hoc network," in *Proc. Int. Conf. Convergence Inf. Technol.*, 2007, pp. 1183–1182.
- [20] [Online]. Available: <http://www.isi.edu/nsnam/ns/>
- [21] D. Jiang, Q. Chen, and L. Delgrossi, "Optimal data rate selection for vehicle safety communications," in *Proc. 5th ACM Int. Workshop VANET*, 2008, pp. 30–38.
- [22] S. Wiethölter, M. Emmelmann, C. Hoene, and A. Wolisz, "TKN EDCA Model for ns-2," Telecommun. Netw. Group, Technische Univ. Berlin, Berlin, Germany, Tech. Rep. TKN-06-003, Jun. 2006.
- [23] P. E. Engelstad and O. N. Osterbo, "Queueing delay analysis of IEEE 802.11e EDCA," in *Proc. WONS*, 2006, pp. 123–133.
- [24] P. E. Engelstad and O. N. Osterbo, "Delay and throughput analysis of IEEE 802.11e EDCA with starvation prediction," in *Proc. IEEE Conf. Local Comput. Netw.*, 2005, pp. 647–655.
- [25] I. Inan, F. Keceli, and E. Ayanoglu, "Saturation throughput analysis of the 802.11e enhanced distributed channel access function," in *Proc. ICC*, 2007, pp. 409–414.
- [26] J. Robinson and T. Randhawa, "Saturation throughput analysis of IEEE 802.11e enhanced distributed coordination function," *IEEE J. Sel. Areas Commun.*, vol. 22, no. 5, pp. 917–928, Jun. 2004.
- [27] H. Wu, X. Wang, Q. Zhang, and X. Shen, "IEEE 802.11e enhanced distributed channel access (EDCA) throughput analysis," in *Proc. IEEE Int. Conf. Commun.*, Jun. 2006, vol. 1, pp. 223–228.
- [28] P. Clifford, K. Duffy, J. Foy, D. J. Leith, and D. Malone, "Modeling 802.11e for data traffic parameter design," in *Proc. 4th Int. Symp. Modeling Optim. Mobile, Ad Hoc, Wireless Netw.*, 2006, pp. 116–125.
- [29] J. W. Tantra, H. F. Chuan, and A. B. Mnaouer, "Throughput and delay analysis of the IEEE 802.11e EDCA saturation," in *Proc. ICC*, 2005, pp. 3450–3454.
- [30] Z. Kong, D. H. K. Tsang, B. Bensaou, and D. Gao, "Performance analysis of IEEE 802.11e contention-based channel access," *IEEE J. Sel. Areas Commun.*, vol. 22, no. 10, pp. 2095–2106, Dec. 2004.
- [31] Z. Tao and S. Panwar, "Throughput and delay analysis for the IEEE 802.11e enhanced distributed channel access," *IEEE Trans. Commun.*, vol. 54, no. 8, pp. 596–603, Apr. 2006.
- [32] S. Pan and J. Wu, "Throughput analysis of IEEE 802.11e EDCA under heterogeneous traffic," *Comput. Commun.*, vol. 32, no. 5, pp. 935–942, Mar. 2009.
- [33] B. Xiang, M. Yu-Ming, and X. Jun, "Performance investigation of IEEE802.11e EDCA under non-saturation condition based on the M/G/1/K model," in *Proc. ICIEA*, 2007, pp. 298–304.
- [34] I. Inan, F. Keceli, and E. Ayanoglu, "Analysis of the 802.11e enhanced distributed channel access function," *IEEE Trans. Commun.*, vol. 57, no. 6, pp. 1753–1764, Jun. 2009.
- [35] Y. Yan and C. Pan, "An improved analytical model for IEEE 802.11e enhanced distributed channel access," in *Proc. ISITC*, 2007, pp. 135–142.
- [36] C.-L. Huang and W. Liao, "Throughput and delay performance of IEEE 802.11e enhanced distributed channel access (EDCA) under saturation condition," *IEEE Trans. Wireless Commun.*, vol. 6, no. 1, pp. 136–145, Jan. 2007.
- [37] D. Xu, T. Sakurai, and H. L. Vu, "An access delay model for IEEE 802.11e EDCA," *IEEE Trans. Mobile Comput.*, vol. 8, no. 2, pp. 261–275, Feb. 2009.
- [38] K. Abboud and W. Zhuang, "Modeling and analysis for emergency messaging delay in vehicular ad hoc networks," in *Proc. IEEE Globecom*, 2009, pp. 1–6.
- [39] F. Hou, L. X. Cai, X. Shen, and J. Huang, "Asynchronous multichannel MAC design with difference-set-based hopping sequences," *IEEE Trans. Veh. Technol.*, vol. 60, no. 4, pp. 1728–1739, May 2011.



**Chong Han** (S'12) received the B.Eng. and M.Eng. degrees in electrical engineering from Harbin Institute of Technology, Harbin, China, in 2005 and 2009, respectively. She is currently working toward the Ph.D. degree with the Centre for Communication Systems Research, Department of Electronic Engineering, University of Surrey, Surrey, U.K.

She participated in the European Union (EU) project PRE-DRIVE C2X, which develops a detailed specification for vehicle to X communication systems and a functionally verified prototype. She is currently involved with the EU project DRIVE C2X, which will lay the foundation for rolling out cooperative systems in Europe with a comprehensive assessment of cooperative systems through field operational tests. Her current research interests are vehicular ad hoc networks, including medium-access-control protocol design and performance analysis, simulation platform, and application development for intelligent transportation systems.



**Mehrdad Dianati** (M'05) received the B.Sc. degree from Sharif University of Technology, Tehran, Iran, in 1992 and the M.Sc. degree from K.N.Toosi University of Technology, Tehran, in 1995, both in electrical engineering, and the Ph.D. degree in electrical and computer engineering from the University of Waterloo, Waterloo, ON, Canada, in 2006.

He was a Hardware/Software Developer and Technical Manager from 1992 to 2002. He is currently a Lecturer (Assistant Professor) with the Centre for Communication Systems Research, Department of Electronic Engineering, University of Surrey, Surrey, U.K.



**Rahim Tafazolli** (SM'07) received the Ph.D. degree from the University of Surrey, Surrey, U.K.

He is currently a Professor of mobile/personal communications and the Director of the Centre for Communication Systems Research, University of Surrey, Surrey, U.K. He has been active in research for more than 25 years. He has authored or coauthored more than 500 papers in refereed international journals and conference proceedings. He is a consultant to many telecommunication companies.

Prof. Tafazolli is a Fellow of the Wireless World Research Forum. He has lectured, chaired, and has been invited as keynote speaker to a number of Institution of Engineering and Technology and IEEE workshops and conferences. He is the Chairman of the European Union Expert Group of NetWorks Technology Platform.



**Xuemin (Sherman) Shen** (M'97–SM'02–F'09) received the B.Sc. degree from Dalian Maritime University, Dalian, China, in 1982 and the M.Sc. and Ph.D. degrees from Rutgers University, Camden, NJ, in 1987 and 1990, respectively, all in electrical engineering.

He is currently a Professor and University Research Chair with the Department of Electrical and Computer Engineering, University of Waterloo, Waterloo, ON, Canada. He was the Associate Chair for Graduate Studies from 2004 to 2008. He is a coauthor of three books and has published more than 500 papers and book chapters in wireless communications and networks, control, and filtering. His research interests include resource management in interconnected wireless/wired networks, wireless network security, wireless body area networks, vehicular ad hoc networks, and sensor networks.

Dr. Shen is an Engineering Institute of Canada Fellow and a Distinguished Lecturer of the IEEE Vehicular Technology and Communications Societies. He is also a registered Professional Engineer in the province of Ontario, Canada. He served as the Technical Program Committee Chair for Fall 2010 IEEE Vehicular Technology Conference (VTC), the Symposia Chair for 2010 IEEE International Conference on Communications (ICC), the Tutorial Chair for the Spring 2011 IEEE VTC and IEEE ICC 2008, the Technical Program Committee Chair for IEEE Globecom 2007, the General Co-Chair for China-com 2007 and QShine 2006, the Chair for the IEEE Communications Society Technical Committee on Wireless Communications, and peer-to-peer Communications and Networking. He also served as a Founding Area Editor for the IEEE TRANSACTIONS ON WIRELESS COMMUNICATIONS; Editor-in-Chief for IEEE NETWORK, PEER-TO-PEER NETWORKING AND APPLICATION, and IET Communications; Associate Editor for the IEEE TRANSACTIONS ON VEHICULAR TECHNOLOGY, COMPUTER NETWORKS, and *ACM/Wireless Networks*, etc.; and a Guest Editor for the IEEE JOURNAL ON SELECTED AREAS IN COMMUNICATIONS, IEEE WIRELESS COMMUNICATIONS, IEEE COMMUNICATIONS MAGAZINE, and *ACM Mobile Networks and Applications*. He received the Excellent Graduate Supervision Award in 2006 and the Outstanding Performance Award in 2004, 2007, and 2010 from the University of Waterloo; the Premier's Research Excellence Award in 2003 from the Province of Ontario; and the Distinguished Performance Award in 2002 and 2007 from the Faculty of Engineering, University of Waterloo.



**Ralf Kernchen** received the Dipl. Inf. (equal to M.Sc. in computer science) degree from the Technical University of Berlin, Berlin, Germany, in 2004 and the Ph.D. degree in mobile communications from the Centre for Communication Systems Research (CCSR), Department of Electronic Engineering, University of Surrey, Surrey, U.K., in 2010.

He was a Research Fellow with CCSR from 2004 to 2011. He has been the Founder and Director of Rulemotion Ltd., London, U.K., since 2011 and has been working on executable business specifications for generative information systems.